TGFβ primes alveolar-like macrophages to induce type I IFN following TLR2 activation.

Sean M. Thomas[,1], Laurisa M. Ankley[,1], Kayla N. Conner[1], Alexander W. Rapp[2], Abigail P. McGee[2], Francois LeSage[2], Christopher D. Tanner[2], Taryn E. Vielma[1], Eleanor C. Scheeres[1], Joshua J. Obar[2, #], Andrew J. Olive[1, #]

[1]Department of Microbiology, Genetics, and Immunology, College of Osteopathic Medicine, Michigan State University, East Lansing, MI
[2]Department of Microbiology & Immunology, Geisel School of Medicine at Dartmouth, Lebanon, NH

[#]Corresponding authors:
Andrew Olive
Michigan State University
College of Osteopathic Medicine
Department of Microbiology, Genetics, and Immunology
East Lansing, MI 48824
E-mail address: oliveand@msu.edu

Joshua J. Obar
Geisel School of Medicine at Dartmouth
Department of Microbiology & Immunology
1 Medical Center Drive
Lebanon, NH 03756
Email: joshua.j.obar@dartmouth.edu

ABSTRACT

Alveolar macrophages (AMs) are key mediators of lung function and are potential targets for therapies during respiratory infections. TGFβ is an important regulator of AM differentiation and maintenance, but how TGFβ directly modulates the innate immune responses of AMs remains unclear. This shortcoming prevents effective targeting of AMs to improve lung function in health and disease. Here we leveraged an optimized *ex vivo* AM model system, fetal-liver derived alveolar-like macrophages (FLAMs), to dissect the role of TGFβ in AMs. Using transcriptional analysis, we first globally defined how TGFβ regulates gene expression of resting FLAMs. We found that TGFβ maintains the baseline metabolic state of AMs by driving lipid metabolism through oxidative phosphorylation and restricting inflammation. To better understand inflammatory regulation in FLAMs, we next directly tested how TGFβ alters the response to TLR2 agonists. While both TGFβ (+) and TGFβ (-) FLAMs robustly responded to TLR2 agonists, we found an unexpected activation of type I interferon (IFN) responses in FLAMs and primary AMs in a TGFβ-dependent manner. Surprisingly, mitochondrial antiviral signaling protein and the interferon regulator factors 3 and 7 were required for IFN production by TLR2 agonists. Together, these data suggest that TGFβ modulates AM metabolic networks and innate immune signaling cascades to control inflammatory pathways in AMs.

INTRODUCTION

The pulmonary space is a specialized environment evolved to facilitate gas exchange and maintain lung function (1, 2). To protect against exposures to airborne microorganisms and particulates, lung alveoli contain a specialized phagocyte population, alveolar macrophages (AMs) (2, 3). These AMs, like many other tissue-resident macrophages, seed the lungs from the fetal liver and serve two primary purposes: to preserve lung homeostasis by maintaining optimal surfactant levels in the lungs and to patrol the alveolar space for inhaled debris, initiating an inflammatory response when necessary (4-6). Given the importance of maintaining pulmonary function, AMs must strictly regulate their inflammatory responses to prevent unnecessary inflammation and tissue damage (7, 8). Compared to other inflammatory macrophages, including bone marrow-derived macrophages (BMDMs), AMs are more hypo-inflammatory against many pathogenic stimuli, a characteristic that is mediated by their distinct ontogeny and the lung environment (8-10). In fact, circulating monocytes that are recruited to the lungs following infection have been shown to adapt to the local environment and take on AM-like phenotypes (11). Two key cytokines, GM-CSF and TGFβ, are known to mediate AM differentiation and functions in the lung environment (6, 12-14). While the role of GM-CSF is better understood due to its importance in preventing pulmonary alveolar proteinosis, how TGFβ directly modulates the AM state and function remains unclear, limiting our ability to target AMs and improve lung function in health and disease.

TGFβ exists as three separate isoforms (TGFβ1-3) that all bind to the same TGFβ coreceptors (TGFβRI, TGFβRII) (15). TGFβ-1 is primarily produced by

macrophages, but in an inactive form, conjugated with a latency-associated peptide (LAP) (16-18). Inactive TGFβ-1 (referred to as TGFβ from here on) is activated following enzymatic, acidic, or receptor-mediated cleavage of the LAP from TGFβ (18, 19). In the lungs, inactive TGFβ is primarily produced by AMs which is then activated by the alveolar epithelial type II cells (AECII) through the activity of the αvβ6 integrin on alveolar epithelial cells (6, 14, 18). Thus, maintaining AMs requires unique interactions between the lung epithelium and disruptions of this environment results in dysregulated pulmonary responses.

In its active form, TGFβ is a versatile cytokine that triggers SMAD complex translocation to the nucleus to drive a multitude of processes, including stem cell differentiation, chemotaxis, and immune regulation, depending on the context in which it is acting (20, 21). Much of this heterogeneity in cellular responses to TGFβ is thought to be due to crosstalk between other transcriptional regulators and epigenetic regulation (22). In the lungs, TGFβ plays critical roles both in lung development and disease. Mice lacking any of the three isoforms of TGFβ or either of the two receptors have varying degrees of deformed lung structure and alveologenesis due to dysregulated interactions between the lung epithelium and mesenchyme during development (23-26). TGFβ is also implicated in the development of idiopathic pulmonary fibrosis (IPF) through its induction of myofibroblast differentiation from lung fibroblasts and suppression of anti-fibrotic factors prostaglandin E2 and hepatocyte growth factor production (27-29). Given the importance of TGFβ to maintain AMs in the lungs, it is essential to better understand how TGFβ modulates the inflammatory potential of AMs.

Fully dissecting the role of TGFβ in AM regulation requires *ex vivo* models that recapitulate key aspects of the lung environment. Recent work by several groups showed that growth of macrophages in both GM-CSF and TGFβ stabilizes the AM-like state for cells grown in culture (30-32). We recently optimized the fetal liver-derived alveolar-like macrophages (FLAMs) model which propagates fetal liver cells in both GM-CSF and TGFβ, allowing for long-term propagation and genetic manipulation of cells that recapitulate many aspects of AM functions (32). Removing TGFβ from these cells results in a loss of the AM-like state such as decreased expression of the key AM transcription factor peroxisome-proliferating activating receptor gamma (PPARγ) and increased expression of the LPS co-receptor CD14. These data suggest that TGFβ not only maintains the AM state, but plays an important role in modulating the inflammatory response of AMs.

In this report we directly examine how TGFβ shapes AM function and inflammatory responses. Using transcriptional analysis, we globally defined how TGFβ regulates the gene expression of resting FLAMs, identifying a key role of TGFβ in maintaining the metabolic state of AMs. In parallel, we characterized how TGFβ shapes the inflammatory response of AMs following the activation of toll-like receptor 2 (TLR2), uncovering an unexpected link between TGFβ, TLR2, and type I interferon (IFN). We found that a range of TLR2 agonists activate type I IFN responses in a TGFβ-dependent manner. Further mechanistic studies found this type I IFN response required the interferon regulatory factor 3 and 7 (IRF3/7) in addition to the mitochondrial antiviral signaling adaptor (MAVS). These data suggest that TGFβ rewires the AMs and

potentiates the activation of unique innate immune signaling not observed in other macrophage populations.

RESULTS

TGFβ drives lipid metabolism, restrains cytokine expression, and maintains FLAMs in the AM-like state.

We previously developed FLAMs as an *ex vivo* model of AMs to understand the mechanistic signals and regulatory networks that maintain cells in the AM-like state (32). TGFβ is a key cytokine needed to maintain AMs *in vivo* and to maintain FLAMs in the AM-like state, yet how TGFβ modulates AM functions and transcriptional networks remains unclear (6, 14, 32). As a first step, we confirmed that TGFβ is required to broadly maintain the AM-like state in FLAMs. FLAMs were grown in GM-CSF in the presence or absence of TGFβ for two-weeks and the expression of the AM-associated surface markers SiglecF and CD14 were quantified by flow cytometry. We observed that FLAMs grown with TGFβ had high expression of SiglecF and CD11a together with low expression of CD14 and CD11b on their surface, while FLAMs grown without TGFβ had opposite pattern of expression with low expression of SiglecF and CD11a and higher expression of CD14 and CD11b (Figure 1A). Since PPARγ is a key transcription factor in AMs and is expressed in both AMs and FLAMs (32, 33), we measured the effect of TGFβ on PPARγ expression. mRNA was isolated from FLAMs grown with and without TGFβ and quantitative RT-PCR was used to determine the expression of *Pparg*. FLAMs grown with TGFβ maintained higher expression of *Pparg*, while cells grown in the absence of TGFβ showed significantly decreased *Pparg* expression (Figure 1B). These data confirm that TGFβ helps maintain FLAMs in an AM-like state, similar to what has been seen with TGFβ's role in differentiation and maintenance of AMs in the lungs (6, 32).

To better understand how TGFβ globally regulates FLAMs, we next conducted whole-transcriptome RNA sequencing analysis on FLAMs grown in the presence and absence of TGFβ. Differential expression analysis identified hundreds of genes that were significantly changed between FLAMs grown with or without TGFβ (Figure 1C and Supplemental Table 1). To globally identify pathways that were uniquely enriched in TGFβ (+) FLAMs, we employed gene set enrichment analysis (GSEA), using a ranked gene list generated from the differential expression analysis (Figure 1D). Among the top hallmark pathways enriched in TGFβ (+) FLAMs were cholesterol homeostasis, TGFβ signaling, and fatty acid metabolism (Figure 1D and Supplemental Figure 1A). Supporting this observation, TGFβ (+) FLAMs contained significantly less intracellular lactate than TGFβ (-) FLAMs (Supplemental Figure 1B). Given that AMs are known to drive PPARγ-dependent lipid metabolism, these data suggest the FLAM transcriptional profile is similar to primary AMs (34, 35). In contrast, pathways enriched in TGFβ (-) FLAMs included the inflammatory response, TNF signaling, and complement (Figure 1D and Supplemental Figure 1A). To directly test similarities between FLAMs and Ams, we compared the expression of a previously published AM gene signature in FLAMs grown with and without TGFβ in addition to primary AMs and peritoneal macrophages (PMs) for the immunological genome project (ImmGen) (Figure 1E and Supplemental Table 2) (36). While there was no significant difference in the expression of this gene signature between AMs and TGFβ (+) FLAMs, there was a significant difference between AMs and TGFβ (-) FLAMs. This further supports that TGFβ maintains FLAMs in an AM-like state. We next directly compared the expression of a subset of genes related to differentially expressed pathways (Figure 1F). We found high expression of lipid

metabolism genes including *Pparg, Acat2*, *Acat3*, and *Fads2* in TGFβ (+) FLAMs. In TGFβ (-) FLAMs, we observed a significant increase in chemokines including *Ccl2*, *Ccl3, Ccl4* and *Cxcl3*. Taken together these data suggest that TGFβ maintains metabolic functions of AMs while restraining basal chemokine expression.

TGFβ mediates a type I IFN response in AMs following Pam3CSK4 Activation.

To understand how TGFβ alters the innate immune response of AMs we next directly tested the response of FLAMs grown with and without TGFβ to inflammatory stimuli. Many bacterial and fungal respiratory infections activate TLR2 signaling during infection (37-41). Thus, we examined whether the activation of TLR2 by the purified agonist Pam3CSK4 (referred to as Pam3) alters the transcriptome of FLAMs in a TGFβ-dependent manner. TGFβ (+) and TGFβ (-) FLAMs were stimulated with Pam3 for 18 hours, then RNA sequencing and differential expression analysis was used to identify changes in the transcriptional landscape. We identified over 700 genes that were significantly altered following Pam3 treatment of TGFβ (+) FLAMs compared to untreated TGFβ (+) FLAMs (Supplementary Figure 2A). We were next curious which pathways were enriched among differentially expressed genes in TGFβ (+) FLAMs compared to TGFβ (-) FLAMs following Pam3 treatment to identify TGFβ-dependent, and perhaps, AM-specific immune signaling (Figure 2A). Using GSEA we found an unexpected enrichment in IFNα response in the TGFβ (+) FLAMs (Figure 2B). When we examined the entire IFNα hallmark pathway, which encompasses the general type I IFN response, across all conditions we only observed robust induction of IFN-related genes in Pam3 treated TGFβ (+) FLAMs (Figure 2C). This finding suggests that TGFβ skews

macrophage responses to drive the activation of type I IFN pathways following Pam3 stimulation.

To further understand the functional outcomes of TLR2 dimerization in TGFβ (+) FLAMs, we next directly examined the normalized reads of IFN related genes. Our transcriptome data showed no expression of any *Ifna* gene or *Ifne* and *Ifng*, but we did observe increased expression of *Ifnb1* and the interferon-stimulated genes (ISGs) *Cxcl10* and *Rsad2* (Figure 2D), suggesting IFNβ is driving the gene signature. We observed similar baseline expression of *Ifnb1*, *Cxcl10* and *Rsad2* between conditions; however, TGFβ (+) FLAMs induced significantly higher expression of all three genes following Pam3 treatment. To corroborate the RNA sequencing results, we compared the secretion of cytokines in resting and Pam3 treated TGFβ (+) and TGFβ (-) FLAMs using an ELISA (Figure 2E). In agreement with our transcriptional results, we observed a significant increase in IFNβ and CXCL10 secretion from Pam3 treated TGFβ (+) FLAMs compared to TGFβ (-) FLAMs. In line with our Pam3-simulated TGFβ (+) FLAMs, we observed that two additional agonists that mimic bacterial or fungal infection, peptidoglycan and zymosan, respectively, resulted in a significant increase in CXCL10 production in TGFβ (+) FLAMs compared to TGFβ (-) FLAMs (Supplemental Figure 2B). In contrast, we observed no significant CXCL10 secretion following activation with depleted zymosan or curdlan (Supplemental Figure 2B), which are pure Dectin-1 ligands (42).

We next confirmed this phenotype occurs in primary murine AMs by isolating cells from the lungs and treating them with increasing Pam3 concentrations, subsequently examining the production of IFNβ by ELISA (Figure 2F). In line with our

results in FLAMs, we observed a significant, dose dependent increase in IFNβ in AMs following treatment with Pam3. To determine if this innate response was AM specific, we next examined primary bone marrow-derived macrophages (BMDMs). FLAMs or BMDMs were grown with or without TGFβ then stimulated with Pam3 and the following day, IFNβ was quantified by ELISA (Figure 2G). We only observed increased IFNβ secretion from FLAMs grown in TGFβ. These data suggest that the effects of TGFβ on TLR2 signaling may be specific to tissue-resident macrophages.

TLR2 engagement in TGFβ (+) FLAMs induces an RLR gene signature and type I IFN production is dependent on MAVS, IRF3, and IRF7.

Since our results suggested that TLR2 agonists drive an increased type I IFN response in TGFβ (+) FLAMs, we next directly tested the role of TLR2 signaling in the induction of the type I IFN response using *Tlr2*$^{(-/-)}$ FLAMs. Wild type and *Tlr2*$^{(-/-)}$ TGFβ (+) FLAMs were stimulated with Pam3 and the following day IFNβ was quantified in the supernatants by ELISA. While wild type TGFβ (+) FLAMs robustly induced IFNβ, this was lost in *Tlr2*$^{(-/-)}$ FLAMs (Figure 3A). This result suggests that TGFβ signaling in FLAMs drives a unique response to TLR2 activation that results in the production of type I IFN.

We next wanted to better understand the pathways driving the TLR2-dependent type I IFN response in TGFβ (+) FLAMs. Examining our transcriptional analysis in Pam3 treated TGFβ (+) and TGFβ (-) FLAMs, we observed a signature GSEA enrichment for RLR signaling (Figure 3A). RLR signaling converges on the mitochondrial antiviral-signaling (MAVS) protein which triggers the activation of the transcription factors

interferon regulatory factors 3 and 7 (IRF3/IRF7) to mediate the transcription of IFNβ (43, 44). To test the role of these genes in controlling TGFβ-dependent type I IFN responses after Pam3 stimulation, we used our previously described CRISPR-Cas9 editing approaches in FLAMs to target *Mavs*, *Irf3* and *Irf7* with individual sgRNAs (32). We first confirmed the functional effects of editing by stimulating TGFβ (+) control, sgMAVS, sgIRF3, and sgIRF7 FLAMs with Poly(I:C) a known activator of MAVS-dependent RLR signaling and measured IFNβ production by ELISA (45). We observed a significant decrease in IFNβ for all three genes targeted suggesting functional defects in RLR signaling (Figure 3B). We next tested the response of these cells to Pam3 and zymosan. The following day secreted IFNβ was quantified by ELISA. Similar to our previous findings, we observed that wild type FLAMs induced IFNβ in response to Pam3 and zymosan (Figure 3C). Surprisingly, we found IFNβ secretion after both Pam3 and zymosan treatment was significantly reduced from the sgMAVS, sgIRF3, and sgIRF7 FLAMs (Figure 3C). These data suggest that TGFβ-dependent, TLR2-mediated type I IFN responses are controlled by MAVS and IRF3/IRF7. To account for possible effects of lentiviral transduction, we next optimized Cas9 mediated editing with ribonuclear protein (RNP). As a proof of principle, we targeted SiglecF and one week following nucleofection examined the surface expression of SiglecF on control and targeted cells by flow cytometry. We found loss of SiglecF on the surface of over 98% of cells on targeted FLAMs compared to controls (Supplemental Figure 3). We next generated *Mavs*-deficient FLAMs using our optimized RNP editing. These *Mavs*-deficient cells did not produce IFNβ in response to Poly(I:C), suggesting functional knockout of MAVS (Figure 3D). In agreement with our lentiviral mutants, we found that genetic loss of *Mavs*

results in a reduction in IFNβ following Pam3 and zymosan stimulation (Figure 3E). Thus, TGFβ-dependent, TLR2-mediated type I IFN responses are controlled by MAVS-dependent signaling.

DISCUSSION

TGFβ signaling is essential for alveolar macrophage (AM) development and homeostasis in the lung environment (6, 14), but how TGFβ signaling regulates the response of AMs to external stimuli remains unclear. Here, we leveraged an *ex vivo* model of AMs, known as FLAMs, to dissect transcriptional changes in AM-like cells that are mediated by TGFβ. We found that while TGFβ restrains a subset of inflammatory pathways, TGFβ also primes AMs for a type I IFN response following treatment with TLR2 agonists. These results suggest that distinct innate immune signaling networks in AMs are regulated by the tissue environment and directly alter the inflammatory response following the activation of TLR2.

While our findings demonstrate an unexpected link between TLR2, MAVS, and type I IFN production in AMs, the cell biology behind how TLR2 activates type I IFN secretion remains an open question. Several pattern recognition receptors (PRRs), including TLR3, TLR7 and TLR9 activate type I IFNs through the activation of IRF3 or IRF7, but these PRRs are localized to the endosome and generally respond to viral ligands (46, 47). In contrast, TLR2 is present on both the surface and in the endosome, similar to TLR4 (48). Previous studies showed that TLR4 signaling through the plasma membrane drives Myd88-dependent NFκβ activation, while signaling through the endosome activates a TRIF-dependent type I IFN response (49). Whether the localization of TLR2 drives the type I IFN response in TGFβ cultured AMs and how the the adaptors, MyD88 and TRIF, contribute to this response will need to be determined. While several previous studies suggest TLR2 can activate type I IFNs, the ligands and cell types capable of this response remain controversial (50-53). For example, Barbalat

et al. showed BMDMs can make type I IFN in response to viral ligands but not bacterial ligands, while Dietrich et al. showed BMDMs can make type I IFN following activation with bacterial ligands (51, 52). Our data support the role of bacterial and fungal TLR2 ligands in activating a type I IFN response in AMs that is dependent on TGFβ signaling. FLAMs grown in the absence of TGFβ did not robustly induce type I IFNs following TLR2 activation. Our genetic studies found that IRF3, IRF7, and MAVS were all required for the TLR2-dependent type I IFN response. This suggests TLR2-mediated type I IFN may activate parallel pathways, one dependent on direct signaling through MyD88/TRIF, and a second dependent on the cytosolic nucleotide sensing pathways dependent on MAVS. Our data support a model where TGFβ primes AMs to enhance the activation of MAVS-dependent type I IFN production.

The mechanisms underlying TGFβ priming of the type I IFN response in AMs remain unknown. TGFβ is known to activate PPARγ and fatty acid oxidation (6), which we confirmed through our transcriptional analysis. Previous studies have linked cellular metabolism and type I IFN production. Both cholesterol biosynthesis and glycolysis byproducts, such as lactate, are known to regulate the magnitude of the type I IFN response in BMDMs (54, 55). Given the increased fatty acid oxidation and mitochondrial function in TGFβ (+) FLAMs, it is possible that TGFβ-dependent changes in lipid metabolism and mitochondrial function directly drive subsequent type I IFN responses following TLR2 activation. Since we observed increased activation of MAVS-dependent type I IFN production following TLR2 stimulation, this suggests the possibility of endogenous cellular ligands such as mitochondrial DNA amplifying the TLR2 response in AMs (56). How changes in mitochondrial dynamics or possibly mitochondrial ROS

generation contribute to the production of IFNβ remains unknown. Future studies will be needed to dissect the role of fatty acid oxidation, oxidative respiration, and mitochondrial damage in driving TLR2-mediated TGFβ-dependent type I IFN responses in AMs.

Our finding that AMs are uniquely programmed by TGFβ to drive a type I IFN response suggests that these specialized resident macrophages differentially activate their inflammatory profiles in the lung environment compared to other macrophages. Understanding the consequences of a type I IFN-skewed response in the lungs is an important line of research for future studies. Type I IFNs are known to be potent regulators of antiviral immunity, suggesting the host response in the lungs is particularly tuned to respond to invading viral pathogens (44). However, type I IFNs also play a key role in controlling respiratory fungal pathogens like *Aspergillus fumigatus* (57). In several disease states however, including Systemic Lupus Erythematosus and tuberculosis, elevated type I IFNs are associated with worse disease, and blocking type I IFN has been shown to improve clinical outcomes (58-60). Our data support the role of type I IFNs as a key initial response to invading pathogens in the lungs and more broadly suggests the balance of type I IFNs can mediate protective or pathologic host responses.

Interestingly, TGFβ is produced in an inactive form by AMs in the lungs and processed into an active form by integrins on lung epithelial cells which then signal back to AMs to maintain their function (6, 18, 19). This interconnected signaling ensures that AMs are properly tuned to the airspace and suggests the lung environment is an important mediator of the enhanced type I response observed in AMs. Better

understanding the underlying mechanisms driving TGFβ-dependent type I IFN may enable the development of therapeutics that modulate the balance of type I IFNs more effectively in the lungs to control infections and prevent autoinflammatory diseases.

MATERIAL & METHODS

Animals

Experimental protocols were approved by the Institutional Animal Care and Use Committees at Michigan State University (animal use form [AUF] no. PROTO202200127) and Dartmouth College (protocol #00002168). All protocols were strictly adhered to throughout the entire study. Six- to 8-wk-old C57BL/6J mice (catalog no. 000664), *Tlr2*$^{(-/-)}$ mice (catalog no. 004650) and Cas9$^{(+)}$ mice (catalog no. 026179) were obtained from The Jackson Laboratory (Bar Harbor, ME). Mice were given free access to food and water under controlled conditions (humidity, 40–55%; lighting, 12-hour light/12-hour dark cycles; and temperature, 24 ± 2°C), as described previously. (32). Pregnant dams at 8–10 week of age and 14–18 gestational days were euthanized to obtain murine fetuses to generated FLAMs. Primary AMs and BMDMs were isolated from male and female mice >10 week of age.

FLAM cell culture

Wild type and *Tlr2*$^{(-/-)}$ FLAMs were isolated as previously described (32) cultured in complete RPMI (Thermo Fisher Scientific) containing 10% FBS (R&D Systems), 1% penicillin-streptomycin (Thermo Fisher Scientific), 30 ng/ml recombinant mouse GM-CSF (PeproTech), and 20 ng/ml recombinant human TGFβ1 (PeproTech) included where indicated. Media were refreshed every 2–3 d. When cells reached 70–90% confluency, they were lifted by incubating for 10 min with 37°C PBS containing 10 mM EDTA, followed by gentle scraping.

AM and BMDM isolation and culture

Mice were euthanized by CO_2 exposure followed by exsanguination via the inferior vena cava. Lungs were lavaged as previously described (32). Cells were then resuspended in RPMI 1640 media containing 30 ng/ml GM-CSF and 20 ng/ml recombinant human TGF-β1 (PeproTech) and plated in untreated 48- or 24-well plates. AMs were lifted from plates using Accutase (BioLegend) and seeded for experiments.

For BMDMs femurs were isolated and bone marrow was harvested following centrifugation of bones cut on one side. Bone marrow was then cultured in complete RPMI 1640 media containing 30ng/ml M-CSF for 7 days in untreated 15 cm dishes. Cells were then split for experiments and treated with or without 20 ng/ml recombinant human TGF-β1 (PeproTech) prior to activation.

Flow Cytometry

To quantify surface expression of AM markers, cells were lifted by gentle scrapping, washed with PBS, and stained with SiglecF-Bv421 (Biolegend, Cat no. 155509) CD11b-APC (Biolegend, Cat no. 101212) CD14-PE-Cy7 (Biolegend, Cat no. 123316) CD11a-PE (Biolegend, Cat no. 153103) (all diluted 1:400 in PBS). Cells were then washed 3 times in PBS and fixed with 1% formaldehyde (J.T. Baker, Cat no. JTB-2106-01) in PBS. Flow cytometry was performed on a BD LSR II or an Attune CytPix at the MSU Flow Cytometry Core, and data were analyzed using FlowJo (Version 10.8.1).

TLR2 activation

Cells were seeded in 24-well or 48-well treated culture plates cells/well and allowed to settle overnight. Cells were treated with Pam3CSK4 25ng/ml (Invivogen, Cat no. tlrl-pms), peptidoglycan from *S. aureus* at 50µg/ml (Invivogen, cat no. tlrl-pgns2), zymosan at 50µg/ml (Invivogen, Cat no. tlrl-zyn), Zymosan Depleted at 50µg/ml (Invivogen, Cat no. tlrl-zyd), Curdlan at 50µg/ml (Invivogen, Cat no. tlrl-curd) or poly I:C at 20µg/mL (Invivogen, Cat no. tlrl-pic-5). Poly I:C was complexed with Lyovec for transfection prior to stimulation.

Cytokine analysis

Where indicated supernatants were analyzed by a Luminex multiplex assay (Eve Technology). In addition, secreted CXCL10 was quantified using the R&D Duoset kit (R&D Sciences) per manufacturer's instructions. Secreted IFNβ was quantified with the LumiKine Xpress mIFN-B 2.0 kit (Invivogen, catalog no luex-mIFNβv2) per manufacturer's instructions. Luminescent signal was detected on a Spark® multimode microplate reader (Tecan).

Lactate Analysis

Intracellular levels of lactate were determined using an L-lactate assay kit (Millipore Sigma, Cat. # MAK329) according to manufacturer instructions.

qRT PCR

RNA from FLAMs was extracted using the Directzol RNA Extraction Kit (Zymo Research, Cat no. R2072) according to the manufacturer's protocol. Quality was assessed using NANODROP. The One-step Syber Green RT-PCR Kit (Qiagen, Cat no. 210215) reagents were used to amplify the RNA and amplifications were monitored using the QuantStudio3 (ThermoFisher, Cat no. A28567).

Pparg Forward: TCGCTGATGCACTGCCTATG

Pparg Reverse: GAGAGGTCCACAGAGCTGATT

Gapdh Forward: AGGTCGGTGTGAACGGATTTG

Gapdh Reverse: TGTAGACCATGTAGTTGAGGTCA

CRISPR-targeted knockouts

Lentiviral-mediated: Single-guide RNA (sgRNA) cloning sgOpti was a gift from Eric Lander and David Sabatini (Addgene plasmid no. 85681) (61). Individual sgRNAs were cloned as previously described (62). In short, sgRNA targeting sequences (*Irf7*: TGTGCGGCCCTTGTACATGA *Mavs*: GAGGACAAACCTCTTGTCTG *Irf3*: GGCTGGACGAGAGCCGAACG) were annealed and phosphorylated, then cloned into a dephosphorylated and BsmBI (New England Biolabs) digested sgOpti. sgRNA constructs were then packaged into lentivirus as previously described and used to transduce early passage $Cas9^+$ FLAMs. Two days later, transductants were selected with puromycin. After 1 week of selection, cells were validated for SiglecF/CD14 expression and used for experimentation.

Ribonuclear protein-mediated:

Three synthetic lypophilized sgRNAs (Synthego) per gene were pooled and prepared according to provided instructions. sgRNAs targeting *Mavs* and NLSx2-Cas9 protein were mixed with FLAMs in P2 primary cell nucleofection solution (Lonza, catalog no. V4XP-2024). Nucleofection was carried out using the 4D-Nucleofector® Core and X Unit (Lonza, catalog no. AAF-1003B and AAF-1003X).

Mavs guide sequences:

#1: AGGAAGCCCGCAGUCGAUCC

#2: UCUUCAAUAAUCUCCAGCGC

#3: UGCAGAUCUGUGAGCUGCCU

Editing efficiency by ICE analysis:

Genomic DNA was isolated from control and target cells using the Qiagen DNeasy Blood and Tissue Kit (Qiagen, catalog no. 69506). Genomic DNA was quantified using a NanoDrop 1000 spectrophotometer (Thermo Scientific, catalog no. 2353-30-0010) and the edited region was amplified using polymerase chain reaction (PCR) and the samples were then sequencing using Sanger Sequencing (Genewiz) and editing efficiency was determined using ICE analysis (Synthego) (63). All cells used have an efficiency >90%.

RNAseq

FLAMs with and without TGFβ were plated in 6-well plates at 1 x 10^6 cells/well and treated with Pam3 as described above for 18 hours. We used the Direct-zol RNA

Extraction Kit (Zymo Research, Cat no. R2072) to extract RNA according to the manufacturer's protocol. Quality was assessed by the MSU Genomics Core using an Agilent 4200 TapeStation System. The Illumina Stranded mRNA Library Prep kit (Illumina, Cat no. 20040534) with IDT for Illumina RNA Unique Dual Index adapters was used for library preparation following the manufacturer's recommendations but using half-volume reactions. Qubit™ dsDNA HS (ThermoFischer Scientific, Cat no. Q32851) and Agilent 4200 TapeStation HS DNA1000 assays (Agilent, Cat no. 5067-5584) were used to measure quality and quantity of the generated libraries. The libraries were pooled in equimolar amounts, and the Invitrogen Collibri Quantification qPCR kit (Invitrogen, Cat no. A38524100) was used to quantify the pooled library. The pool was loaded onto 2 lanes of a NovaSeq S4 flow cell, and sequencing was performed in a 2x150 bp paired end format using a NovaSeq 6000 v1.5 100-cycle reagent kit (Illumina, Cat no. 20028316). Base calling was performed with Illumina Real Time Analysis (RTA; Version 3.4.4), and the output of RTA was demultiplexed and converted to the FastQ format with Illumina Bcl2fastq (Version 2.20.0).

RNAseq analysis was completed using the MSU High Performance Computing Center (HPCC). FastQC (Version 0.11.7) was used to assess read quality. Bowtie2 (Version 2.4.1) (64) with default settings was used to map reads with the GRCm39 mouse reference genome. Aligned reads counts were assessed using FeatureCounts from the Subread package (Version 2.0.0) (65). Differential gene expression analysis was conducted using the DESeq2 package (Version 1.36.0) (66) in R (Version 4.2.1).

All raw sequencing data, raw read counts, and normalized read counts will be available through the NCBI Gene Expression Omnibus database.

Core AM upregulated signature genes were compared between FLAMs grown with and without TGFβ from our study and AMs and peritoneal macrophages from ImmGen (GSE122108 (6, 36)). Raw counts were compiled and normalized in DESeq2. A box plot was generated in GraphPad Prism using normalized counts for core AM upregulated signature genes. Gene set enrichment analysis (GSEA) was used to identify enriched pathways in the RNA-seq dataset. Genes in the indicated comparisons were ranked using DeSeq2, and the “GSEA preranked” function was used to complete functional enrichment using default settings for hallmark pathways from mice. We acknowledge our use of the gene set enrichment analysis, GSEA software, and Molecular Signature Database (MSigDB) (59) (http://www.broad.mit.edu/gsea/).

ACKNOWLEDGMENTS

This work was supported by grants from the National Institutes of Health: R01 AI139133 (J.J.O), R35 GM146795 (A.J.O.) and R01 AI165618 (A.J.O.). A.W.R. was supported by the Dartmouth College Molecular Microbiology & Pathogenesis Program (NIH/NIAID T32 AI007519). A.P.M. was supported by the Dartmouth College Immunology Training Program (NIH/NIAID T32 AI007363). F.L. was supported by the Dartmouth College Cystic Fibrosis Training Program (NIH/NIAID T32 HL134598) and CFRDP Training Core from the Cystic Fibrosis Foundation. The Attune CytPix, located in the MSU Flow Cytometry Core Facility, is supported by the Equipment Grants Program, award #2022-70410-38419, from the U.S. Department of Agriculture (USDA), National Institute of Food and Agriculture (NIFA).

FIGURE LEGENDS

Figure 1. TGFβ drives lipid metabolism, restrains chemokine expression, and maintains FLAMs in the AM-like state. (A) The expression of the indicated surface markers was quantified by flow cytometry from TGFβ (+) and (-) FLAMs and are shown as representative histograms (left) and the quantified mean fluorescence intensity (right). Each point represents a technical replicate from one representative experiment of 3. **p<0.01 by unpaired students t-test. **(B)** *Pparg* expression was quantified by qRT-PCR using $2^{(-\Delta\Delta CT)}$ relative to GAPDH in untreated TGFβ (+) and (-) FLAMs. Each point represents a technical replicate from one representative experiment of 3. **p<0.01 by unpaired students t-test. **(C)** Differentially expressed genes were identified between untreated TGFβ (+) and (-) FLAMs. Red points represent significantly under-expressed genes and blue points represent significantly overexpressed genes between TGFβ (+) and (-) FLAMs. Each point represents the mean of three biological replicates from one experiment. DeSeq2 was used to determine significance using the adjusted p-value to account for multiple hypothesis testing. **(D)** Shown are the top hallmark pathways enriched in TGFβ (+) and (-) FLAMs. **(E)** Normalized counts of core AM genes were compared among TGFβ (+) and (-) FLAMs and previously published datasets from ImmGen (ImmGen PM and ImmGen AM; accession GSE122108, https://www.ncbi.nlm.nih.gov/geo/query/acc.cgi?acc=GSE122108). The box plot shows the median with quartiles representing the 10th to 90th percentile range of the data within that cell type. Each point represents the mean normalized counts of an individual gene. The Mann–Whitney *U* test was used to make statistical comparisons between each cell type and to compare medians.
(F) Gene expression was quantified from normalized counts for key genes important in lipid metabolism, inflammation, and TGFβ signaling. Each point represents a technical replicate from one experiment. *** adjusted p-value <0.001 using DeSeq2 analysis.

Figure 2. TGFβ mediates type I IFN responses during TLR2 activation. (A) TGFβ (+) and (-) FLAMs were stimulated with 50ng/ml Pam3 and 18 hours later differentially expressed genes were identified between TGFβ (+) and (-) FLAMs left untreated or treated with Pam3 treated for 18 hours. Leading edge analysis of differentially expressed genes identified the IFN-alpha response hallmark pathway comparing Pam3 activation in TGFβ (+) and (-) FLAMs **(B)** Expression of genes representing the IFNα hallmark pathway between TGFβ (+) and (-) FLAMs that have or have not been treated with Pam3. Each column of 3 biological replicates represents an experimental condition from one experiment. **(C)** Normalized read counts from *Ifnb*, *Rsad2* and *Cxcl10* from Pam3 RNA sequencing experiment. *** adjusted p-value <0.001 using DeSeq2 analysis. **(D)** TGFβ (+) and (-) FLAMs were stimulated with Pam3 for 24hrs. Supernatants were collected for quantification of IFNβ and CXCL10 by ELISA **(E)** Wild type FLAMs or *Tlr2*$^{(-/-)}$ FLAMs, were stimulated with Pam3 for 24hrs. Secreted IFNβ was quantified by ELISA. Each point represents data from a single well from one representative experiment of three. ****p<0.0001 ** p<0.01 by one-way ANOVA with a Tukey post-hoc test for multiple comparisons. **(F)** TGFβ (+) FLAMs or primary AMs from C57BL6/J mice were stimulated with the indicated concentrations of Pam3 and IFNβ was quantified by ELISA the following day. Shown is one representative experiment of

three each containing 3 replicates per experiment. **p<0.01 ***p<.001 by one-way ANOVA with a Tukey post-hoc test for multiple comparisons. **(G)** FLAMs or BMDMs grown with or without TGFβ were stimulated with Pam3 for 24 hours and IFNβ was quantified by ELISA. Shown is one representative experiment of two containing three replicates per group.

Figure 3. MAVS contributes to TGFβ-dependent type I IFN responses. (A) Leading edge analysis of differentially expressed genes identified RLR signaling comparing Pam3 activation in TGFβ (+) and (-) FLAMs. **(B)** Wild type, sgMAVS, sgIRF3, and sgIRF7 FLAMs were stimulated with Poly(I:C) for 24hrs. Secreted IFNβ was quantified by ELISA. Shown is a representative experiment of three with at least 3 samples per group. **(C)** Wild type, sgMAVS, sgIRF3, and sgIRF7 FLAMs were stimulated with Pam3 or Zymosan for 24hrs. Secreted IFNβ was quantified by ELISA. Shown is a representative experiment of three with at least 3 samples per group **(D)** Wild type or *Mavs* KO FLAMs were stimulated with poly I:C for 24hrs. Secreted IFNβ was quantified by ELISA. **(E)** Wild type or *Mavs* KO FLAMs were stimulated with Pam3 or Zymosan for 24hrs. Secreted IFNβ was quantified by ELISA. Each point represents data from a single well from one representative experiment of four. *** p<0.001, ** p<0.01 by one-way ANOVA with a Tukey post-hoc test for multiple comparisons.

Supplemental Figure 1. (A) Gene expression was quantified from normalized counts for key genes important in lipid metabolism, inflammation, and TGFβ signaling between TGFβ FLAMs (+) and (-) at homeostasis. **(B)** Lactate levels produced over 18 hours were quantified from cell lysates of FLAMs grown with or without TGFβ. Shown are representative data of two experiments containing 3-5 replicates per group. Each point represents data from a single well, with the bar showing the mean ± one standard deviation. ****p<.0001 by unpaired student t-test

Supplemental Figure 2. (A) Differentially expressed genes were identified between TGFβ FLAMs (+) with and without Pam3 treatment for 18 hours. Red points represent under-expressed genes and blue points represent overexpressed genes following Pam3 activation. Each point represents the mean of three biological replicates from one experiment. **(B)** TGFβ (+) and (-) FLAMs were stimulated with 50ng/ml peptidoglycan, zymosan, depleted zymosan, or curdlan for 24hrs. CXCL10 was quantified by ELISA.

Supplemental Figure 3. Surface levels of SiglecF were quantified by flow cytometry on control FLAMs or FLAMs transfected with RNPs targeted SiglecF. Shown is a representative overlaid flow cytometry plot with control cells (Red) and SiglecF KO cells (Blue) of SiglecF staining.

LITERATURE CITED

1. Hsia CC, Hyde DM, Weibel ER. 2016. Lung Structure and the Intrinsic Challenges of Gas Exchange. Compr Physiol 6:827-95.

2. Kopf M, Schneider C, Nobs SP. 2015. The development and function of lung-resident macrophages and dendritic cells. Nat Immunol 16:36-44.

3. Branchett WJ, Lloyd CM. 2019. Regulatory cytokine function in the respiratory tract. Mucosal Immunol 12:589-600.

4. Wu Y, Hirschi KK. 2020. Tissue-Resident Macrophage Development and Function. Front Cell Dev Biol 8:617879.

5. van de Laar L, Saelens W, De Prijck S, Martens L, Scott CL, Van Isterdael G, Hoffmann E, Beyaert R, Saeys Y, Lambrecht BN, Guilliams M. 2016. Yolk Sac Macrophages, Fetal Liver, and Adult Monocytes Can Colonize an Empty Niche and Develop into Functional Tissue-Resident Macrophages. Immunity 44:755-68.

6. Yu X, Buttgereit A, Lelios I, Utz SG, Cansever D, Becher B, Greter M. 2017. The Cytokine TGF-beta Promotes the Development and Homeostasis of Alveolar Macrophages. Immunity 47:903-912 e4.

7. Ardain A, Marakalala MJ, Leslie A. 2020. Tissue-resident innate immunity in the lung. Immunology 159:245-256.

8. Rothchild AC, Olson GS, Nemeth J, Amon LM, Mai D, Gold ES, Diercks AH, Aderem A. 2019. Alveolar macrophages generate a noncanonical NRF2-driven transcriptional response to Mycobacterium tuberculosis in vivo. Sci Immunol 4.

9. Pisu D, Huang L, Grenier JK, Russell DG. 2020. Dual RNA-Seq of Mtb-Infected Macrophages In Vivo Reveals Ontologically Distinct Host-Pathogen Interactions. Cell Rep 30:335-350 e4.

10. Huang L, Nazarova EV, Tan S, Liu Y, Russell DG. 2018. Growth of Mycobacterium tuberculosis in vivo segregates with host macrophage metabolism and ontogeny. J Exp Med 215:1135-1152.

11. Aegerter H, Kulikauskaite J, Crotta S, Patel H, Kelly G, Hessel EM, Mack M, Beinke S, Wack A. 2020. Influenza-induced monocyte-derived alveolar macrophages confer prolonged antibacterial protection. Nat Immunol 21:145-157.

12. Suzuki T, Sakagami T, Rubin BK, Nogee LM, Wood RE, Zimmerman SL, Smolarek T, Dishop MK, Wert SE, Whitsett JA, Grabowski G, Carey BC, Stevens C, van der Loo JC, Trapnell BC. 2008. Familial pulmonary alveolar proteinosis caused by mutations in CSF2RA. J Exp Med 205:2703-10.

13. Schneider C, Nobs SP, Kurrer M, Rehrauer H, Thiele C, Kopf M. 2014. Induction of the nuclear receptor PPAR-gamma by the cytokine GM-CSF is critical for the differentiation of fetal monocytes into alveolar macrophages. Nat Immunol 15:1026-37.

14. Branchett WJ, Cook J, Oliver RA, Bruno N, Walker SA, Stolting H, Mack M, O'Garra A, Saglani S, Lloyd CM. 2021. Airway macrophage-intrinsic TGF-beta1 regulates pulmonary immunity during early-life allergen exposure. J Allergy Clin Immunol 147:1892-1906.

15. Tzavlaki K, Moustakas A. 2020. TGF-beta Signaling. Biomolecules 10.

16. Nunes I, Shapiro RL, Rifkin DB. 1995. Characterization of latent TGF-beta activation by murine peritoneal macrophages. J Immunol 155:1450-9.

17. Dennis PA, Rifkin DB. 1991. Cellular activation of latent transforming growth factor beta requires binding to the cation-independent mannose 6-phosphate/insulin-like growth factor type II receptor. Proc Natl Acad Sci U S A 88:580-4.

18. Annes JP, Rifkin DB, Munger JS. 2002. The integrin alphaVbeta6 binds and activates latent TGFbeta3. FEBS Lett 511:65-8.

19. Gleizes PE, Munger JS, Nunes I, Harpel JG, Mazzieri R, Noguera I, Rifkin DB. 1997. TGF-beta latency: biological significance and mechanisms of activation. Stem Cells 15:190-7.

20. Gong D, Shi W, Yi SJ, Chen H, Groffen J, Heisterkamp N. 2012. TGFbeta signaling plays a critical role in promoting alternative macrophage activation. BMC Immunol 13:31.

21. Gratchev A. 2017. TGF-beta signalling in tumour associated macrophages. Immunobiology 222:75-81.

22. Chung JY, Chan MK, Li JS, Chan AS, Tang PC, Leung KT, To KF, Lan HY, Tang PM. 2021. TGF-beta Signaling: From Tissue Fibrosis to Tumor Microenvironment. Int J Mol Sci 22.

23. Chen H, Zhuang F, Liu YH, Xu B, Del Moral P, Deng W, Chai Y, Kolb M, Gauldie J, Warburton D, Moses HL, Shi W. 2008. TGF-beta receptor II in epithelia versus mesenchyme plays distinct roles in the developing lung. Eur Respir J 32:285-95.

24. Sanford LP, Ormsby I, Gittenberger-de Groot AC, Sariola H, Friedman R, Boivin GP, Cardell EL, Doetschman T. 1997. TGFbeta2 knockout mice have multiple developmental defects that are non-overlapping with other TGFbeta knockout phenotypes. Development 124:2659-70.

25. Kulkarni AB, Huh CG, Becker D, Geiser A, Lyght M, Flanders KC, Roberts AB, Sporn MB, Ward JM, Karlsson S. 1993. Transforming growth factor beta 1 null mutation in mice causes excessive inflammatory response and early death. Proc Natl Acad Sci U S A 90:770-4.

26. Shull MM, Ormsby I, Kier AB, Pawlowski S, Diebold RJ, Yin M, Allen R, Sidman C, Proetzel G, Calvin D, et al. 1992. Targeted disruption of the mouse transforming growth factor-beta 1 gene results in multifocal inflammatory disease. Nature 359:693-9.

27. Willis BC, Liebler JM, Luby-Phelps K, Nicholson AG, Crandall ED, du Bois RM, Borok Z. 2005. Induction of epithelial-mesenchymal transition in alveolar epithelial cells by transforming growth factor-beta1: potential role in idiopathic pulmonary fibrosis. Am J Pathol 166:1321-32.

28. Frangogiannis N. 2020. Transforming growth factor-beta in tissue fibrosis. J Exp Med 217:e20190103.

29. Garrison G, Huang SK, Okunishi K, Scott JP, Kumar Penke LR, Scruggs AM, Peters-Golden M. 2013. Reversal of myofibroblast differentiation by prostaglandin E(2). Am J Respir Cell Mol Biol 48:550-8.

30. Gorki AD, Symmank D, Zahalka S, Lakovits K, Hladik A, Langer B, Maurer B, Sexl V, Kain R, Knapp S. 2022. Murine Ex Vivo Cultured Alveolar Macrophages Provide a Novel Tool to Study Tissue-Resident Macrophage Behavior and Function. Am J Respir Cell Mol Biol 66:64-75.

31. Luo M, Lai W, He Z, Wu L. 2021. Development of an Optimized Culture System for Generating Mouse Alveolar Macrophage-like Cells. J Immunol 207:1683-1693.

32. Thomas ST, Wierenga KA, Pestka JJ, Olive AJ. 2022. Fetal Liver-Derived Alveolar-like Macrophages: A Self-Replicating Ex Vivo Model of Alveolar Macrophages for Functional Genetic Studies. Immunohorizons 6:156-169.

33. Smith MR, Standiford TJ, Reddy RC. 2007. PPARs in alveolar macrophage biology. PPAR Res 2007:23812.

34. Baker AD, Malur A, Barna BP, Ghosh S, Kavuru MS, Malur AG, Thomassen MJ. 2010. Targeted PPARgamma deficiency in alveolar macrophages disrupts surfactant catabolism. J Lipid Res 51:1325-31.

35. Remmerie A, Scott CL. 2018. Macrophages and lipid metabolism. Cell Immunol 330:27-42.

36. Heng TS, Painter MW, Immunological Genome Project C. 2008. The Immunological Genome Project: networks of gene expression in immune cells. Nat Immunol 9:1091-4.

37. Oliveira-Nascimento L, Massari P, Wetzler LM. 2012. The Role of TLR2 in Infection and Immunity. Front Immunol 3:79.

38. Gopalakrishnan A, Salgame P. 2016. Toll-like receptor 2 in host defense against Mycobacterium tuberculosis: to be or not to be-that is the question. Curr Opin Immunol 42:76-82.

39. Rubino I, Coste A, Le Roy D, Roger T, Jaton K, Boeckh M, Monod M, Latge JP, Calandra T, Bochud PY. 2012. Species-specific recognition of Aspergillus fumigatus by Toll-like receptor 1 and Toll-like receptor 6. J Infect Dis 205:944-54.

40. Buckland KF, O'Connor E, Murray LA, Hogaboam CM. 2008. Toll like receptor-2 modulates both innate and adaptive immune responses during chronic fungal asthma in mice. Inflamm Res 57:379-87.

41. Balloy V, Si-Tahar M, Takeuchi O, Philippe B, Nahori MA, Tanguy M, Huerre M, Akira S, Latge JP, Chignard M. 2005. Involvement of toll-like receptor 2 in experimental invasive pulmonary aspergillosis. Infect Immun 73:5420-5.

42. Goodridge HS, Wolf AJ, Underhill DM. 2009. Beta-glucan recognition by the innate immune system. Immunol Rev 230:38-50.

43. Ivashkiv LB, Donlin LT. 2014. Regulation of type I interferon responses. Nat Rev Immunol 14:36-49.

44. McNab F, Mayer-Barber K, Sher A, Wack A, O'Garra A. 2015. Type I interferons in infectious disease. Nat Rev Immunol 15:87-103.

45. Wang X, Caffrey-Carr AK, Liu KW, Espinosa V, Croteau W, Dhingra S, Rivera A, Cramer RA, Obar JJ. 2020. MDA5 Is an Essential Sensor of a Pathogen-Associated Molecular Pattern Associated with Vitality That Is Necessary for Host Resistance against Aspergillus fumigatus. J Immunol 205:3058-3070.

46. Thompson MR, Kaminski JJ, Kurt-Jones EA, Fitzgerald KA. 2011. Pattern recognition receptors and the innate immune response to viral infection. Viruses 3:920-40.

47. Li D, Wu M. 2021. Pattern recognition receptors in health and diseases. Signal Transduct Target Ther 6:291.

48. Kawai T, Akira S. 2011. Toll-like receptors and their crosstalk with other innate receptors in infection and immunity. Immunity 34:637-50.

49. Toshchakov V, Jones BW, Perera PY, Thomas K, Cody MJ, Zhang S, Williams BR, Major J, Hamilton TA, Fenton MJ, Vogel SN. 2002. TLR4, but not TLR2, mediates IFN-beta-induced STAT1alpha/beta-dependent gene expression in macrophages. Nat Immunol 3:392-8.

50. Stack J, Doyle SL, Connolly DJ, Reinert LS, O'Keeffe KM, McLoughlin RM, Paludan SR, Bowie AG. 2014. TRAM is required for TLR2 endosomal signaling to type I IFN induction. J Immunol 193:6090-102.

51. Dietrich N, Lienenklaus S, Weiss S, Gekara NO. 2010. Murine toll-like receptor 2 activation induces type I interferon responses from endolysosomal compartments. PLoS One 5:e10250.

52. Barbalat R, Lau L, Locksley RM, Barton GM. 2009. Toll-like receptor 2 on inflammatory monocytes induces type I interferon in response to viral but not bacterial ligands. Nat Immunol 10:1200-7.

53. Oosenbrug T, van de Graaff MJ, Haks MC, van Kasteren S, Ressing ME. 2020. An alternative model for type I interferon induction downstream of human TLR2. J Biol Chem 295:14325-14342.

54. York AG, Williams KJ, Argus JP, Zhou QD, Brar G, Vergnes L, Gray EE, Zhen A, Wu NC, Yamada DH, Cunningham CR, Tarling EJ, Wilks MQ, Casero D, Gray DH, Yu AK, Wang ES, Brooks DG, Sun R, Kitchen SG, Wu TT, Reue K, Stetson DB, Bensinger SJ. 2015. Limiting Cholesterol Biosynthetic Flux Spontaneously Engages Type I IFN Signaling. Cell 163:1716-29.

55. Zhang W, Wang G, Xu ZG, Tu H, Hu F, Dai J, Chang Y, Chen Y, Lu Y, Zeng H, Cai Z, Han F, Xu C, Jin G, Sun L, Pan BS, Lai SW, Hsu CC, Xu J, Chen ZZ, Li HY, Seth P, Hu J, Zhang X, Li H, Lin HK. 2019. Lactate Is a Natural Suppressor of RLR Signaling by Targeting MAVS. Cell 178:176-189 e15.

56. West AP, Shadel GS. 2017. Mitochondrial DNA in innate immune responses and inflammatory pathology. Nat Rev Immunol 17:363-375.

57. Espinosa V, Dutta O, McElrath C, Du P, Chang YJ, Cicciarelli B, Pitler A, Whitehead I, Obar JJ, Durbin JE, Kotenko SV, Rivera A. 2017. Type III interferon is a critical regulator of innate antifungal immunity. Sci Immunol 2.

58. Mayer-Barber KD, Andrade BB, Oland SD, Amaral EP, Barber DL, Gonzales J, Derrick SC, Shi R, Kumar NP, Wei W, Yuan X, Zhang G, Cai Y, Babu S, Catalfamo M, Salazar AM, Via LE, Barry CE, 3rd, Sher A. 2014. Host-directed therapy of tuberculosis based on interleukin-1 and type I interferon crosstalk. Nature 511:99-103.

59. Ji DX, Witt KC, Kotov DI, Margolis SR, Louie A, Chevee V, Chen KJ, Gaidt MM, Dhaliwal HS, Lee AY, Nishimura SL, Zamboni DS, Kramnik I, Portnoy DA, Darwin KH, Vance RE. 2021. Role of the transcriptional regulator SP140 in resistance to bacterial infections via repression of type I interferons. Elife 10.

60. Postal M, Vivaldo JF, Fernandez-Ruiz R, Paredes JL, Appenzeller S, Niewold TB. 2020. Type I interferon in the pathogenesis of systemic lupus erythematosus. Curr Opin Immunol 67:87-94.

61. Fulco CP, Munschauer M, Anyoha R, Munson G, Grossman SR, Perez EM, Kane M, Cleary B, Lander ES, Engreitz JM. 2016. Systematic mapping of functional enhancer-promoter connections with CRISPR interference. Science 354:769-773.

62. Shalem O, Sanjana NE, Hartenian E, Shi X, Scott DA, Mikkelson T, Heckl D, Ebert BL, Root DE, Doench JG, Zhang F. 2014. Genome-scale CRISPR-Cas9 knockout screening in human cells. Science 343:84-87.

63. Conant D, Hsiau T, Rossi N, Oki J, Maures T, Waite K, Yang J, Joshi S, Kelso R, Holden K, Enzmann BL, Stoner R. 2022. Inference of CRISPR Edits from Sanger Trace Data. CRISPR J 5:123-130.

64. Langmead B, Salzberg SL. 2012. Fast gapped-read alignment with Bowtie 2. Nat Methods 9:357-9.

65. Liao Y, Smyth GK, Shi W. 2014. featureCounts: an efficient general purpose program for assigning sequence reads to genomic features. Bioinformatics 30:923-30.

66. Love MI, Huber W, Anders S. 2014. Moderated estimation of fold change and dispersion for RNA-seq data with DESeq2. Genome Biol 15:550.

Figure 1

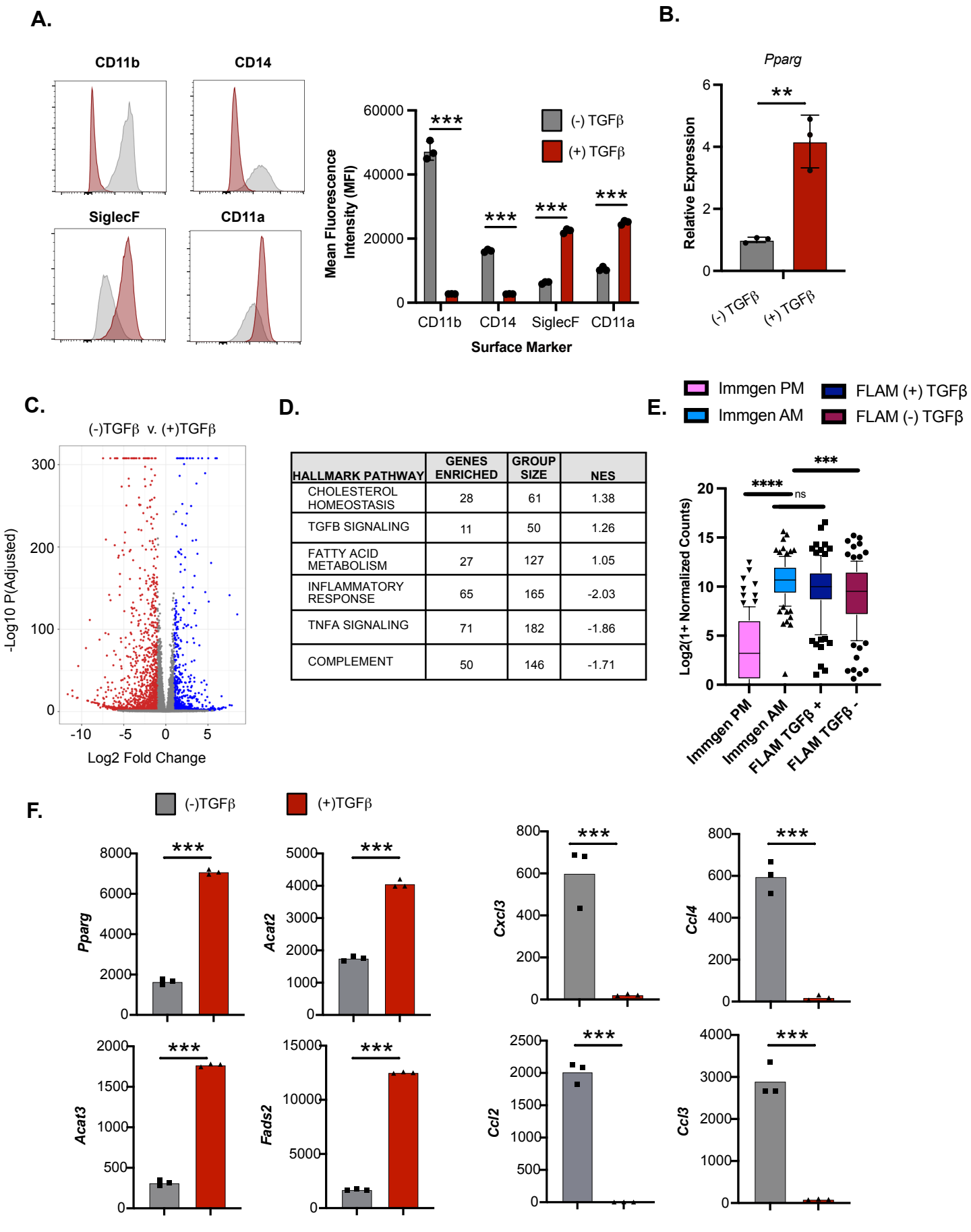

HALLMARK PATHWAY	GENES ENRICHED	GROUP SIZE	NES
CHOLESTEROL HOMEOSTASIS	28	61	1.38
TGFB SIGNALING	11	50	1.26
FATTY ACID METABOLISM	27	127	1.05
INFLAMMATORY RESPONSE	65	165	-2.03
TNFA SIGNALING	71	182	-1.86
COMPLEMENT	50	146	-1.71

Figure 2

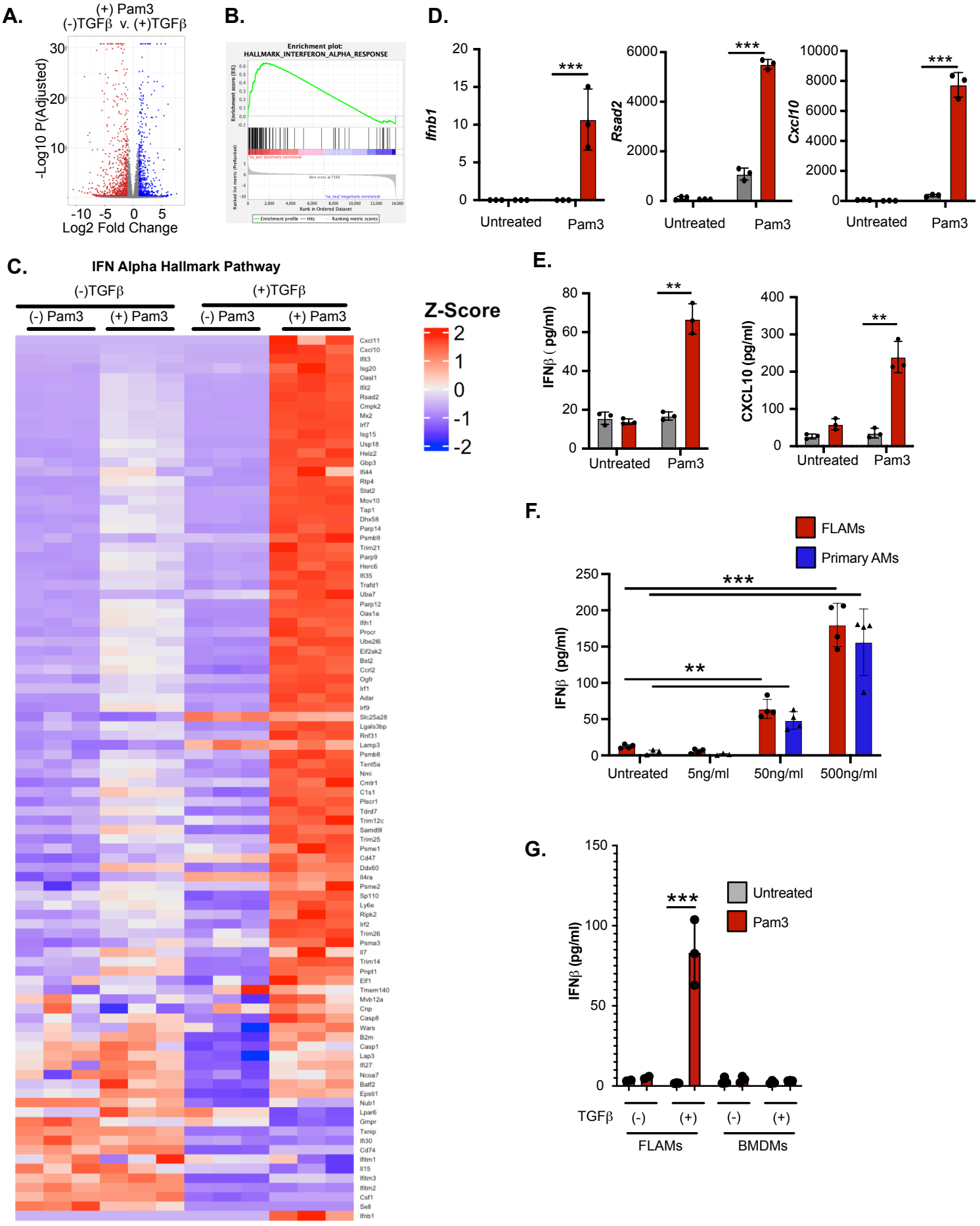

Figure 3